Solubility of Fluoromethemoglobin S: Effect of Phosphate and Temperature on Polymerization

Marielle E. Yohe, Karen M. Sheffield, and Ishita Mukerji
Molecular Biology and Biochemistry Department, Molecular Biophysics Program, Wesleyan University, Middletown, Connecticut 06459-0175 USA

ABSTRACT The polymerization properties of the fully liganded fluoromet derivative of hemoglobin S (FmetHb S) were investigated by electron microscopy and absorption spectroscopy. Polymerization progress curves, as measured by increasing sample turbidity at 700 nm, exhibit a delay time (t_d) consistent with the double nucleation mechanism. The pattern of fiber growth, as monitored by electron microscopy, is also indicative of a heterogeneous nucleation process, and dimensions of the fibers were found to be comparable to that of deoxyHb S. The polymerization rate constant ($1/t_d$) depends exponentially on Hb S concentration, and the size of the homogeneous and heterogeneous nuclei also depend on FmetHb S concentration. As for deoxyHb S, higher concentrations of protein and phosphate favor fiber formation, while lower temperatures inhibit polymerization. Solubility experiments reveal, however, that eight times more FmetHb S is required for polymerization. The current studies further show that reaction order is independent of phosphate concentration if Hb S activity and not concentration is considered. The allosteric effector, inositol hexaphosphate (IHP), promotes fiber formation, and temperature-dependent reaggregation of FmetHb S suggests that IHP stabilizes pregelation aggregates. These studies show that FmetHb S resembles deoxyHb S in many of its polymerization properties; however, IHP-bound FmetHb S potentially provides a unique avenue for future studies of the early stages of Hb S polymerization and the effect of tertiary and quaternary protein structure on the polymerization process.

INTRODUCTION

The single point mutation (β6 Glu→Val) in human hemoglobin leads to the association of sickle cell hemoglobin (Hb S) tetramers into long fibers. The polymerization is driven by a hydrophobic interaction between the β6 Val and an acceptor pocket formed by the β85 Phe and β88 Leu residues on a different tetramer. This association primarily occurs in the unliganded or deoxy form, in which the quaternary rearrangement of the subunits upon deoxygenation leads to the exposure of the β85 Phe and β88 Leu residues and their subsequent interaction with the β6 Val (Padlan and Love, 1985; Harrington et al., 1997).

The mechanism of sickle cell hemoglobin polymerization has been studied extensively by a number of methods, including absorption spectroscopy, electron microscopy, light scattering, and birefringence (Eaton and Hofrichter, 1990, and references therein). Polymerization kinetics are characterized by a delay time, a period during which aggregation cannot be measured. This delay time depends strongly on the concentration of protein present and the temperature of the solution. In the initial stages of polymerization, the exponential growth of fibers in conjunction with the delay time has been well described by a double nucleation mechanism. In this mechanism the initial period of fiber formation is dominated by a homogeneous nucleation process, in which a certain number of Hb tetramers must associate before assembly becomes a spontaneous process. During the period of exponential growth, heterogeneous nucleation dominates, in which fibers grow on the surface of preexisting fibers (Ferrone et al., 1985b). In terms of the pathology of sickle cell disease, the length of the delay time is critical. A delay time that is longer than the circulation time allows cells to become reoxygenated at the lungs before sickling can occur (Mozzarelli et al., 1987).

The influence of ligation state on tetramer association into fibers has been investigated through the use of other hemoglobin mutants (Bookchin and Nagel, 1971) and modified heme derivatives (Adachi et al., 1991). Polymerization of deoxy-cyanomet hybrids suggests that the quaternary state of hemoglobin was the dominant factor influencing the propensity toward polymerization (Bookchin and Nagel, 1971). Later studies of Ni(II)-Fe(II) hybrids suggested that tertiary structure also influences the polymerization, as these hybrids did not polymerize as readily as deoxyHb S (Adachi et al., 1991). Under physiological conditions fiber formation can occur in solutions that are 85% oxygenated (Adachi and Asakura, 1982); thus, understanding the ability of liganded Hb to form fibers is relevant for elucidating the mechanism of fiber formation in vivo. Liganded Hb S derivatives can also be incorporated into Hb S fibers (Adachi and Asakura, 1982), indicating that ligation state can influence the polymerization process.

In this study we report on the formation of fibers, using the fully-liganded fluoromet derivative of hemoglobin S. In this derivative form the heme iron is oxidized ($Fe^{2+} \rightarrow Fe^{3+}$), and a fluoride ion occupies the sixth coordination position normally reserved for oxygen (Perutz et al., 1974).

Received for publication 9 June 1999 and in final form 7 March 2000.

Address reprint requests to Dr. Ishita Mukerji, Hall-Atwater-Shanklin Laboratories, Department of Molecular Biology and Biochemistry, Wesleyan University, Middletown, CT 06459-0175. Tel.: 860-685-2422; Fax: 860-685-2141; E-mail: imukerji@wesleyan.edu.

0006-3495/00/06/3218/09 $2.00

This liganded Hb S can be induced to form fibers by the addition of the allosteric effector inositol hexaphosphate (IHP) and thus allows the examination of polymerization as a function of allosteric state independent of the liganded state. X-ray crystallography has shown that the deoxy quaternary structure of this hemoglobin derivative is very similar to that of Hb A (Fermi and Perutz, 1977). UV resonance Raman measurements have further revealed that the tertiary structure of the fluoromet derivative is slightly perturbed relative to deoxy Hb A, although the quaternary structure was unchanged as measured by the $\alpha_1\beta_2$ intersubunit H-bonds (Jayaraman et al., 1993; Sokolov and Mukerji, 1998; Juszczak et al., 1998). The tertiary structure perturbation was associated with a displacement of the E-helix as a consequence of the liganded nature of the heme.

Despite these differences in tertiary structure, upon conversion to the T-quaternary state we observe polymerization of FmetHb S. Characterization of the FmetHb S fibers by electron microscopy shows that the fibers are comparable in dimension to those formed by deoxyHb S. As for deoxyHb S, the diameter and the length of the fibers increase with time (Wellems and Josephs, 1979; Briehl et al., 1990). Analysis of the kinetic progress curves obtained from turbidity measurements demonstrates that polymerization is dependent on hemoglobin concentration, sample temperature, phosphate concentration, and ionic strength. The initial stages of polymerization are well described by the double nucleation model, and the analysis indicates that the sizes of homogeneous and heterogeneous nuclei are dependent on protein concentration. Further evidence for heterogeneous nucleation is clearly observed in the electron micrographs of the FmetHb S fibers.

These analyses suggest that, consistent with earlier observations (Bookchin and Nagel, 1971; Adachi et al., 1991), the quaternary state of the protein is the dominant factor influencing polymerization. Because polymerization is dependent upon IHP addition, the T quaternary state is required for FmetHb S polymerization. The current characterization of FmetHb S fibers indicates that, despite the perturbation of tertiary structure and the presence of four ligands, the polymerization can be described by the same heterogeneous nucleation mechanism as deoxyHb S.

MATERIALS AND METHODS

Hemoglobin S preparation

Hb S was isolated from the blood of SS and AS patients, following the procedure of Antonini and Brunori (1971). 2,3-Diphosphoglycerate was removed from the hemoglobin on a Sephadex G-25 column equilibrated with 10 mM Tris-HCl, 0.1 M NaCl (pH 8) (Riggs, 1981). Hb S was purified on a Whatman DE-52 column by gradient elution from 50 mM Tris-acetate, pH 8.3, to 50 mM Tris-acetate, pH 7.3 (Huisman and Dozy, 1965). The purified Hb S was characterized by nondenaturing polyacrylamide gel electrophoresis, exposed to carbon monoxide, and frozen at 77 K for storage (Riggs, 1981).

Preparation of fluorometHb

Hb S or Hb A was converted to the fluoromet form, following the procedure of Jayaraman et al. (1993). The concentration of fluoromethemoglobin was determined spectrophotometrically by using the heme extinction coefficients, $\epsilon_{606} = 10.3\ \mathrm{mM}^{-1}\ \mathrm{cm}^{-1}$ and $\epsilon_{490} = 10.9\ \mathrm{mM}^{-1}\ \mathrm{cm}^{-1}$ (Di Iorio, 1981).

Turbidity experiments

Kinetic experiments with fluoromethemoglobin S were carried out in 1-mm-path-length optical glass cuvettes. The reference for the experiments was FmetHb A. IHP was added to the samples, in a stock solution of 0.55 M in the appropriate phosphate buffer (0.15–1.0 M phosphate, pH 6.5) and 0.25 M NaF. IHP was added to the Hb solutions on ice, vortexed, and then quickly transferred to glass cuvettes on ice. Turbidity measurements were performed on a Beckman DU 650 spectrophotometer. A Beckman High-Performance Temperature Controller was used to maintain the temperature of the sample holder at 10°C. The sample compartment was continuously flushed with dry N_2 gas to prevent condensation on the cuvettes. The optical density at 700 nm (A700) was monitored as a function of time. All turbidity measurements were performed at 25°C unless otherwise noted. The time required for thermal equilibration (~30 s) was measured directly in the cuvette with a copper-constantan thermocouple. Because of the time required for thermal equilibration, delay times shorter than 2 min are not reported. Data analysis was performed with the program Origin (Microcal). The turbidity progress curves were fit using the following equation:

$$A700 = \frac{A700_o - A700_{max}}{1 + e^{(t-t_d)/dt}} + A700_{max},$$

where A700 is the absorbance or turbidity of the sample at time t, and $t = 0$ is the moment of the temperature jump (Adachi and Asakura, 1979). $A700_o$ is the initial turbidity, $A700_{max}$ is the maximum turbidity, and t_d is the delay time. The initial 10% of the turbidity progress curves were also fit to the equation $A700(t) = A700_o + [A_f\,(A700_{max} - A700_o)][\cosh(Bt) - 1]$, in which A_f, B, and $A700_o$ were adjustable parameters. A_f is defined as $A/(c_o - c(\infty))$, where $c(\infty)$ is concentration of polymerized hemoglobin at equilibrium. $A700(t)$ is the optical density at 700 nm as a function of time, $A700_o$ is the initial optical density at 700 nm, and $A700_{max}$ is the maximum optical density observed (Ferrone et al., 1985a).

Solubility experiments

IHP was added to solutions of FmetHb S to a final concentration of 140 mM. The solutions were maintained at room temperature overnight. To separate the fibers from the solution, samples were centrifuged for 20 min at 10,000 rpm in an Eppendorf 5415C benchtop microcentrifuge. A 2-μl aliquot of the supernatant was diluted into 1 ml of a fluoride-containing phosphate buffer, and the concentration of tetramers in the supernatant was determined spectrophotometrically. This measurement was done a total of four times on each sample, and the results were averaged.

Preparation of electron microscopy grids

Negatively stained samples for electron microscopy were prepared by applying 2 μl of 0.75 mM FmetHb S solution to a carbon support film over a 300-mesh gold grid. The solution was drawn to a thin layer and fixed with ~5 μl of 2% (w/v) glutaraldehyde. After a 5-min incubation, the fixative was drawn to a thin layer, and the sample was negatively stained with ~5 μl of 2% (w/v) phosphotungstate (pH 7.0). After 1 min, the stain was drawn to a thin layer. Grids were viewed within 24 h of preparation, using a Zeiss 10A tunneling electron microscope. The buffer solution consisted

of 0.25 M potassium phosphate (pH 6.5), 0.25 M NaF, and 140 mM IHP, except for the 0.5-h grid, which was prepared with 120 mM IHP.

RESULTS

Size and shape of FmetHb S fibers

FmetHb S tetramers were converted to the T-quaternary state by the addition of the allosteric effector IHP. The change in quaternary state conformation was verified by UV-Vis absorption spectroscopy. The T-R difference spectrum (data not shown) exhibits maxima at 403, 490, and 606 nm, consistent with the conversion of tetramers to the T quaternary state (Perutz et al., 1974).

The presence of fibers was established by electron microscopy. In these studies fiber formation was followed as a function of time, and the dimensions of the fibers were determined (Fig. 1). The onset of polymerization corresponded to the addition of IHP to the solution. After 30 min, the association of tetramers into fibers is clearly observed (Fig. 1 *A*). In addition, fibers have already started to align to form larger fibers with diameters as large as 250 nm. The majority of the fibers observed have diameters ranging from 30 to 100 nm. The occurrence of heterogeneous nucleation, that is, the formation of a new fiber on a preexisting fiber, can already be detected. Fibers, observed in gels or in sickled red blood cells, typically have a diameter of 21 nm and are variable in length (Wellems and Josephs, 1979).

The progression of fiber formation was also monitored by electron microscopy. One hour after IHP addition, fibers associated into larger domains, as shown in Fig. 1 *B*. The smallest fiber had a diameter of 25 $\pm$ 2 nm, and the largest fiber domains were $\sim$400 nm in diameter. Twenty-four hours after the onset of polymerization the fibers had increased noticeably in diameter and length (Fig. 1 *C*). The smallest fiber domains observed were 77 nm in diameter, and the largest domains were 2 μm in diameter. The largest fiber domains observed in gel and sickled cells were several millimeters in diameter and were formed by slow heating over a time scale of hours. Because of their relative opacity, larger domains are difficult to observe. Smaller domains, which can be prepared by either chemical reduction or laser photolysis, had a size of 1 μm or less in diameter (Eaton and Hofrichter, 1990). Differences in size may result from the manner in which the fibers were prepared, although the fibers observed in the current study were well within the size ranges previously reported for fibers of deoxyHb S. In addition, the increase in dimension with time is consistent with the expected pattern of fiber growth (Briehl et al., 1990). At all time points a branched pattern of gel formation is observed, demonstrating that heterogeneous nucleation is occurring. We cannot rule out the possibility that because of the bound ligand and allosteric effector, the association of the fibers into larger domains is not the same as that for deoxyHb S. The observed domains are not as regular as

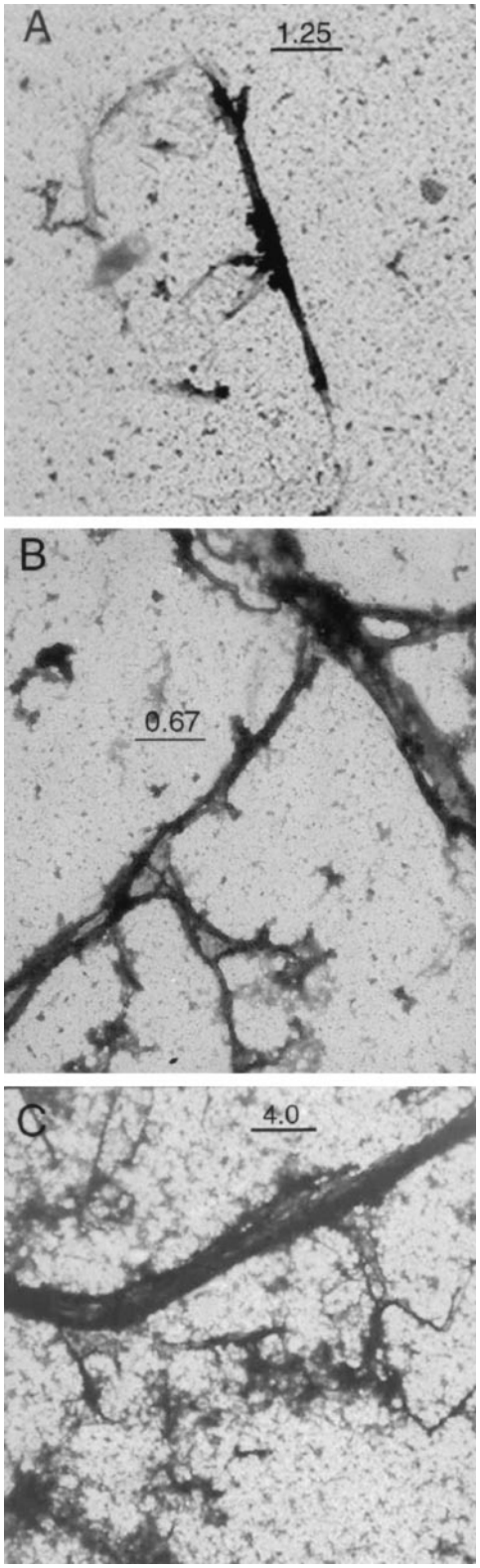

FIGURE 1 FmetHb S fiber formation monitored by electron microscopy. (*A*) Thirty minutes after initiation of polymerization. (*B*) One hour after initiation of polymerization. (*C*) Twenty-four hours after initiation of polymerization. All size scales are shown in microns. Fiber formation was initiated with IHP, and fibers were prepared from a buffer containing 0.25 M potassium phosphate (pH 6.5) and 0.25 M NaF.

those observed with deoxyHb S, and the characteristic herringbone pattern associated with the formation of fibers is not readily detected (Wellems and Josephs, 1979). A more detailed analysis is required to determine if FmetHb S is forming the characteristic 14-stranded structure observed for deoxyHb S.

Dependence of maximum turbidity on HbS concentration

Polymerization of FmetHb S was studied by monitoring the optical density of polymerizing solutions at 700 nm. At this wavelength the heme prosthetic groups have no significant absorption, and the increasing absorption observed as a function of polymerization results from the increasing turbidity of the sample. In Fig. 2 progress curves of polymerization as monitored by sample turbidity are shown for five different FmetHb S concentrations. At all concentrations shown, FmetHb S polymerizes with a clear demonstration of a delay time (t_d) or period during which the absorbance of the sample remains zero, followed by a period during which the absorbance increases rapidly, signifying rapid polymerization. In addition, the maximum turbidity observed increases with increasing Hb S concentration. This behavior is similar to that of deoxyHb S and is indicative that the amount of polymers observed strongly depends on protein concentration (Hofrichter et al., 1974; Adachi and Asakura, 1979). The increase in signal amplitude, coupled with the shortening of the delay time, is suggestive of an increase in polymer concentration with increasing protein concentration.

Polymerization, in terms of sample turbidity, was also monitored as a function of phosphate concentration (Fig. 3). Five different phosphate concentrations ranging from 0.15 to 1.0 M were examined. At lower phosphate concentrations, a higher concentration of protein is needed for polymer formation; however, at these concentrations polymers form to the same extent as estimated from the maximum turbidity. For example, at 0.15 M phosphate a FmetHb S concentration of 2.1 mM (13.44 g/100 ml) is required to observe a maximum turbidity of 1.0, whereas at 0.75 M phosphate, a concentration of only 1.1 mM (7.04 g/100 ml) is need to achieve a maximum turbidity of 1.0. Although the protein concentration requirements for FmetHb S polymerization are phosphate dependent, polymer concentration as estimated from signal amplitude appears to be independent of phosphate concentration.

This relative increase in polymer concentration with increasing protein concentration is consistent with the measured supersaturation ratio ($S = c_o/c_s$; c_o = initial concentration; c_s = solution concentration at equilibrium), as shown in Table 1 for a phosphate concentration of 0.75 M. For a FmetHbS concentration of 0.7 mM, S is 4.6 and increases to 8.2 when the protein concentration is increased to 1.1 mM. This increase in S is reflective of a 1.7-fold increase in polymer concentration with the increasing total protein concentration. In the turbidity experiments, the signal amplitude ($A700_{max}$) increases from 0.2 to 1.0 as the total protein concentration is increased from 0.7 to 1.1 mM; therefore the increase in signal amplitude appears to be related to the overall increase in polymer concentration.

We have also examined the effect of other salts on FmetHb S polymerization and find that at the same ionic strength, polymerization is not observed to the same degree in the presence of either sulfate or nitrate (data not shown). Furthermore, IHP is requisite for FmetHb S polymerization, indicating that the T-state must be present to observe fibers. Under the same conditions, FmetHb A does not form any kind of detectable aggregate (data not shown). Based upon

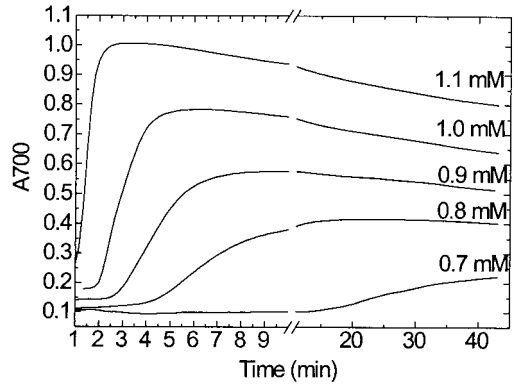

FIGURE 2 The effect of hemoglobin concentration on FmetHb S polymerization. Sample turbidity was monitored by measuring the absorbance at 700 nm. Samples were in a 0.44 M sodium fluoride, 0.14 M IHP, 0.75 M potassium phosphate (pH 6.5) buffer. Polymerization was initiated by increasing the sample temperature from 10°C to 25°C.

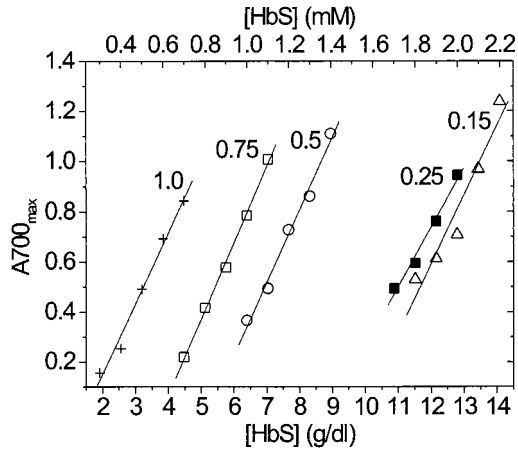

FIGURE 3 The relationship between maximum turbidity and initial FmetHb S concentration. Turbidity was monitored at five different phosphate concentrations: 0.15 (△), 0.25 (■), 0.5 (○), 0.75 (□), and 1.0 (+) M phosphate. Sample conditions are the same as in Fig. 2.

TABLE 1 Homogeneous and heterogeneous nuclei size for FmetHb S

$[\text{FmetHb S}]_0$ (mM)	$[\text{FmetHb S}]_s$* (mM)	A_f	B	$S^\dagger$	$i^{*\ddagger}$	$j^{*\S}$
0.7	0.191	0.00179	0.29	4.59	9.67	10.33
0.8	0.193	0.01332	0.94	5.43	8.71	9.30
0.9	0.199	0.00064	2.81	6.22	8.06	8.61
1.0	0.195	0.001558	3.18	7.41	7.35	7.85
1.1	0.203	0.00174	4.34	8.18	7.01	7.48

*$[\text{FmetHb S}]_s$ is the concentration of the soluble phase of FmetHb S after equilibrium has been reached.

†$S = (\gamma_0 * [\text{FmetHb S}]_0)/(\gamma_s * [\text{FmetHb S}]_s)$.

‡$i^* = -(4RT + \delta_1\mu_{PC})/(RT \ln S)$; δ_1 describes the fraction of intermolecular bonds in the nucleus relative to the infinite polymer and is derived from structural considerations of the polymer; μ_{PC} is the contribution to the chemical potential of a monomer in an infinite polymer from intermolecular bonds (Ferrone et al., 1985b).

§$j^* = -[\delta_1\mu_{PC} + 3RT]/(RT \ln S') = i^* + 1/(\ln S)$ (Ferrone et al., 1985b).

these observations, we conclude that the process we are detecting is specific to Hb S, requires formation of the T-state, and is facilitated by phosphate.

Solubility of FmetHb S

Because of the pronounced effect phosphate concentration can have on Hb S solubility, we have examined the solubility of FmetHb S (Table 1) and compared it with that of deoxyHb S, using the same concentrations of phosphate, NaF, and IHP. DeoxyHb S solubility is 0.15 g/dl under these conditions, and FmetHb S solubility is 1.22 g/dl; thus FmetHb S is approximately eight times more soluble than deoxyHb S. A previous study of half-liganded Ni (II)-Fe(II) hybrid Hb measured solubility differences of 12 and six times relative to the deoxygenated hybrid (Adachi et al., 1991). These results indicate that despite formation of the T-state, the presence of ligands increases the solubility of Hb S. In the case of FmetHb S, the increased solubility may result from the tetraliganded nature of the hemoglobin as well as incomplete formation of the T allosteric state by some of the tetramers (Jayaraman et al., 1993).

Dependence of the delay time (t_d) on HbS and phosphate concentration

The rate of gelation also depends exponentially on Hb S concentration (Fig. 2)—higher concentrations of HbS lead to a shortening of the delay time. The observation of an exponential dependence further confirms that the increase in sample turbidity results from polymerization and not "salting out" of the protein at higher concentration. A linear dependence can be extracted by plotting the logarithm of the reciprocal delay time ($\log 1/t_d$) versus the logarithm of the protein concentration ($\log [\text{Hb S}]$) (Fig. 4). This dependence has been examined at five different phosphate buffer concentrations (0.15–1.0 M), and at all phosphate concentrations a linear relationship was obtained. The concentration of IHP, the organic phosphate used to induce T-state formation, was kept constant at 0.14 M. From these plots the relationship between Hb S concentration and the delay time appears to be dependent on phosphate concentration—the delay time is more steeply dependent on Hb S concentration at lower phosphate concentrations. A slope or n value of 13.5 is obtained at a phosphate concentration of 0.25 M, while a slope of 6.3 is obtained at 1.0 M phosphate. The slope or n value has been related to the size of the homogeneous nucleus, where the delay time is interpreted to be the time required for nucleus formation (Hofrichter et al., 1974). Using a simple homogeneous nucleation model, the nucleus size can be related to the reaction order, as the nucleus size will correspond approximately to the number of rate-limiting addition reactions needed to form the critical nucleus (Hofrichter et al., 1974; Behe and Englander, 1978).

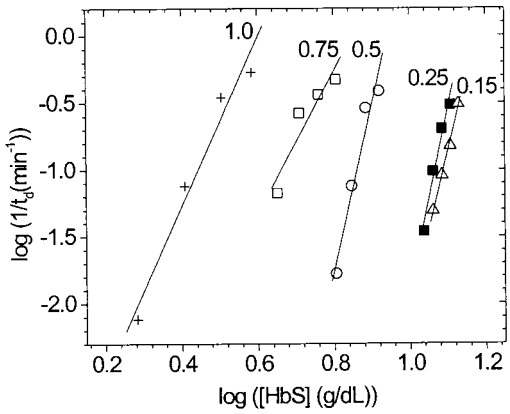

FIGURE 4 The relationship between delay time and FmetHb S concentration. Delay times were monitored at five different phosphate concentrations: 0.15 (△), 0.25 (■), 0.5 (○), 0.75 (□), and 1.0 (+) M phosphate. The log of reciprocal delay time versus log Hb S concentration yields a linear relationship with the slope (n) as indicated. Delay times are taken from data shown in Fig. 3.

In previous studies, the delay time was found to depend on the 30th power of the deoxyHb S concentration in solutions of low ionic strength (Hofrichter et al., 1974, 1976), whereas, a 13th-power dependence was observed at 1.0 M phosphate (Eaton and Hofrichter, 1990). For deoxyHb S the n value depends linearly on phosphate concentration, where smaller values were observed at higher phosphate concentrations (Adachi and Asakura, 1979). In our studies, the n value also has a linear dependence on phosphate concentration and can be described as $n = -16p + 32$. For this analysis, the total phosphate concentration was considered, including the considerable contribution from the allosteric effector, IHP, present in the sample. This phosphate dependence is analogous to that obtained by

Adachi and Asakura (1979) for deoxyHb S ($n = -16p + 31.5$), where p is the total phosphate concentration. The linear relationship suggests that in the absence of phosphate or at low ionic strength the n value is 32, which is similar to the 30th power dependence observed by Hofrichter and co-workers (1974).

The relatively high concentrations of Hb S used in these studies argues that the nonideal nature of these solutions should be considered (Ross and Minton, 1977). To assess the dependence of t_d on phosphate concentration without incorporating the excluded volume effect of increasing protein concentration, we have plotted $\log(1/t_d)$ versus log Hb S activity (Fig. 5). For this plot Hb S activity was calculated using the activity coefficients as determined by Minton (1983). If the nonideality of the solution is taken into account, then the apparent dependence of t_d on phosphate concentration is removed. For data taken at five different phosphate concentrations the average slope or reaction order is 5.8 ± 1.5. Previous estimations of the reaction order by this methodology yielded a value of 9 for deoxy Hb S (Behe and Englander, 1978), which is ~30% higher than the value obtained in this study. This difference in reaction order may result from the relatively large differences in ionic strength used for the two studies. We also observe that IHP may play a role in facilitating nucleus formation and thus potentially reduces the reaction order (see below). Nevertheless, in contrast to the findings of Adachi and Asakura (1979), we observe that the reaction order is independent of phosphate concentration, and the apparent dependence results from the increased nonideality of the solutions.

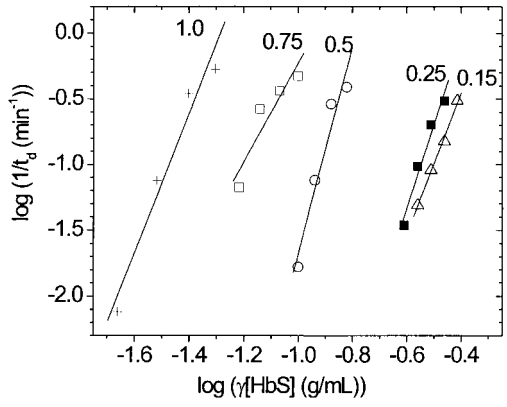

FIGURE 5 The dependence of the delay time on FmetHb S activity. Delay times were monitored at five different phosphate concentrations: 0.15 (△), 0.25 (■), 0.5 (○), 0.75 (□), and 1.0 (+) M phosphate. The log of reciprocal delay time versus log Hb S activity yields a linear relationship with the slope (n) as indicated. Delay times are taken from data shown in Fig. 3.

Temperature dependence of FmetHb S polymerization

The temperature dependence of polymerization was also examined, using a constant concentration of Hb S, phosphate buffer, and IHP. The aggregation of the polymers was found to be strongly temperature dependent (Fig. 6), as the maximum turbidity increased with increasing temperature. This effect is consistent with an increased concentration of polymers at higher temperature. The delay time decreases with increasing temperature, indicating that the rate constant for polymerization is reduced at higher temperatures. This shortening of the delay time with increased temperature was also observed with deoxyHb S (Hofrichter et al., 1974; Adachi and Asakura, 1979) and was associated with an increased facility for aggregation at higher temperature. The rate of gelation can be analyzed in terms of its temperature dependence to extract an activation energy for the process.

Fig. 7 depicts the temperature-dependent analysis of FmetHb S polymerization and shows that ($\log 1/t_d$) depends linearly on $1/T$. Analysis of the slope from 15°C to 35°C yields an activation energy of 18 ± 2 kcal/mol. Previous determinations of the activation energy for deoxyHb S gave values ranging from 20 kcal/mol at high temperature to 50 kcal/mol at temperatures near 20°C. We observe that the curve bends and is suggestive of a lower activation energy at higher temperatures. This behavior is consistent with that of deoxyHb S and suggests that the activation energy is temperature dependent, reflecting the increased propensity for polymerization at higher temperature (Hofrichter et al., 1974; Adachi and Asakura, 1979). The decreased value for the activation energy observed for FmetHb S relative to deoxyHb S possibly results from the presence of stabilized aggregates (vide infra).

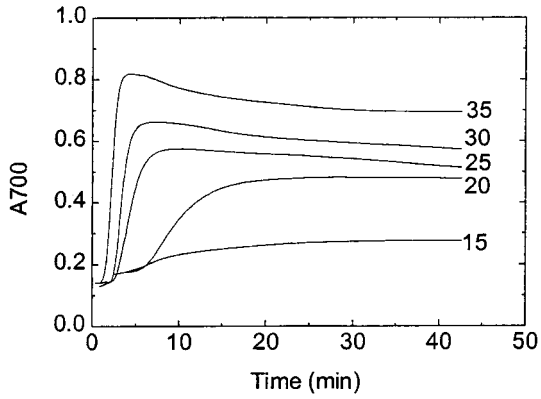

FIGURE 6 Temperature dependence of FmetHb S polymerization. Sample turbidity was monitored at five different temperatures: 15°C, 20°C, 25°C, 30°C, 35°C. Sample conditions are the same as in Fig. 2.

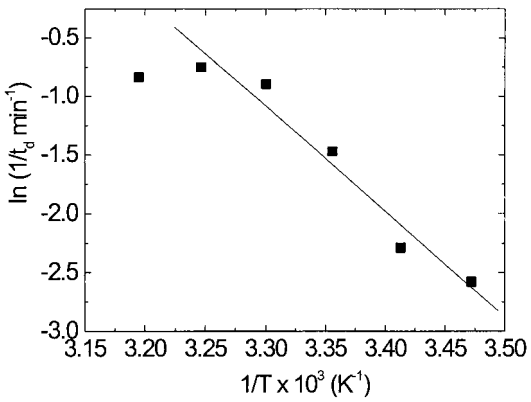

FIGURE 7 The dependence of the delay time on temperature. Delay times were monitored at six different temperatures: 15°C, 20°C, 25°C, 30°C, 35°C, 40°C. Delay times are taken from data shown in Fig. 6. From the slope the activation energy was determined to be 18 ± 2 kcal/mol.

Temperature-dependent reversibility of FmetHb S polymerization

Deaggregation of deoxy Hb S fibers can be accomplished by oxygenation, dilution, or a reduction in temperature. In the case of FmetHb S deaggregation is performed either by dilution or by removal of IHP. We have observed that extensive dialysis to remove IHP leads to a melting of the fibers, and the resultant solutions can be induced to form fibers with comparable delay times by the reintroduction of IHP (data not shown). Thus, under these conditions, the polymerization of FmetHb S is fully reversible.

We have monitored the reaggregation of FmetHb S fibers after cooling the sample to induce deaggregation (Fig. 8). In deoxyHb S the reaggregation delay time strongly depends on the time between deaggregation and reaggregation, for which an interval of 120 min was required before the original delay time was observed (Adachi and Asakura, 1979). For FmetHb S, however, even after 120 min of cooling, a delay time is not observed (Fig. 8), which is indicative that FmetHb S polymerization, reversible by dilution and removal of IHP, is not fully reversible by temperature. This absence of a delay time in reaggregation can be explained by the presence of stabilized aggregates that facilitate formation of the critical nucleus needed for heterogeneous nucleation. The presence of aggregates in a melted polymer solution was recently confirmed by UV Raman measurements (L. Sokolov, personal communication). As this stabilization occurs only when IHP is not removed from the solution, we further suggest that the allosteric effector IHP and not FmetHb S is responsible for the stabilized aggregates. Other allosteric effectors, such as bezafibrate and clofibric acid, also stabilize the T-state and enhance the sickling of red blood cells (Mehanna and Abraham, 1990). We propose that this enhanced sickling could result from the stabilization of aggregates as observed with IHP.

DISCUSSION

We have investigated the mechanics and kinetics of polymer formation of FmetHb S to understand the effect of ligands on the polymerization process and to probe its suitability as a model system for studying Hb S polymerization. We have observed that the polymerization properties of this modified Hb S are comparable to those of deoxyHb S, specifically with respect to phosphate concentration, temperature, and Hb S concentration. This observation suggests that the quaternary state and not the liganded state dominates the polymerization process. FmetHb S is eight times more soluble than deoxyHb S, and we suggest that this increased solubility results from the tetraliganded nature of the derivative. We note that the overall size of the fibers, as determined by electron microscopy, is comparable to that of deoxyHb S fibers. The present studies do not specifically examine the structure of the FmetHb S fibers but record the overall dimension as a function of time. The association pattern of the individual strands and the actual structure of the fibers formed by FmetHb S require more detailed electron microscopy studies.

Polymerization of FmetHb S is well described by the double nucleation mechanism. This mechanism, originally proposed by Ferrone et al. (1985b) for deoxyHb S, accounts for the autocatalytic nature of the kinetic progress curves. Polymerization is described by a two-step process, in which formation of the critical nucleus is the rate-limiting step, resulting in the initial delay time portion of the curve when polymerization is not detectable. Heterogeneous nucleation occurs in the second phase, in which the surfaces of preexisting polymers become nucleation sites. As the polymers increase in size, the surface area for heterogeneous nucleation increases, leading to the exponential growth of fibers once polymerization begins to occur (Eaton and Hofrichter, 1990).

Linearization of the rate equations describing the double nucleation model leads to the following relatively simple relation: $A700(t) = A700_o + [A_f(A700_{max} - A700_o)] \cdot [\cosh(Bt) - 1]$ (Ferrone et al., 1985a). Analysis of the initial 10% of our progress curves, using the above expression, yields excellent fits, verifying that this model adequately describes the data (fits not shown). Because of the limited concentration range of our experiments, however, the experimentally determined A and B parameters (Table 1) could not be used to determine the kinetic and thermodynamic parameters needed to calculate nucleus size. Therefore, the sizes of the homogeneous and heterogeneous nuclei were calculated using the experimentally determined supersaturation ratio ($S = c_o/c_s$, where c_s is solution concentration at equilibrium) for FmetHb S and the kinetic and thermodynamic parameters determined by Ferrone et al. (1985b) for deoxyHb S. The calculated nucleation sizes (Table 1) are comparable in magnitude to those determined for deoxyHb S (Ferrone et al., 1985b). Given the differences

in sample concentration and the relatively high concentration of phosphate used in our study, a direct comparison is not appropriate. Of significance, however, is the dependence of the nucleus size on concentration, which is predicted from the double nucleation model. As expected, the sizes of the heterogeneous and homogeneous nuclei (Table 1) decrease with increasing protein concentration. These results suggest that the mechanism of FmetHb S polymerization is similar to that of deoxyHb S, and, consequently, results obtained with FmetHb S polymers may be used to understand the polymerization of deoxyHb S.

Our studies of FmetHb S have further revealed an interesting role for phosphate in the polymerization process. Similar to previously reported results, we observe that phosphate facilitates polymerization and cannot be functionally replaced with other salts (Ross and Subramanian, 1978; Adachi and Asakura, 1979; Fasanmade, 1996). We find, however, that the reaction order or the dependence of the polymerization rate on protein concentration is independent of phosphate concentration, if protein activity and not concentration is considered. Although similar to the value determined by Behe and Englander (1978) for deoxyHb S, the reaction order obtained for FmetHb S is smaller. We attribute the reduced reaction order and potentially smaller nucleus size for FmetHb S to the increased stabilization of the nucleus by the organic phosphate effector IHP. Current understanding of the nucleation process would suggest that in the first stages of the process sequential addition of monomers is thermodynamically unfavorable. This process becomes more favorable, however, as the stabilization due to intermolecular bond formation becomes greater than the entropy loss associated with the reduction in motional freedom (Eaton and Hofrichter, 1990).

The temperature-dependent deaggregation and reaggregation kinetics (Fig. 8) in the presence of IHP are suggestive of the increased stabilization of fibers and gelation aggregates, which leads to the absence of a delay time in the reaggregation process. This process is IHP dependent, as the reaction is fully reversible by dilution or dialysis. These results suggest that the presence of IHP facilitates aggregation by potentially stabilizing aggregates. We suggest that IHP reduces the free energy barrier to nucleus formation by stabilizing the formation of intermolecular bonds. The smaller activation energy (18 kcal/mol) observed for FmetHb S is consistent with a model in which bound IHP stabilizes intermolecular contacts and lowers the energetic barriers to nucleus formation and subsequent polymerization. The determined activation energy is within error the same as that determined for deoxyHb S at higher temperature. For FmetHb S, the polymerization activation energy is also temperature dependent, implying that the factors affecting the reaction rate are the same for the two forms of Hb S. Some evidence suggests that IHP binds to more than one site on the protein (Coletta et al., 1993). Our results do not discriminate between the two putative IHP binding sites and cannot address the matter of which site is responsible for the increased stabilization.

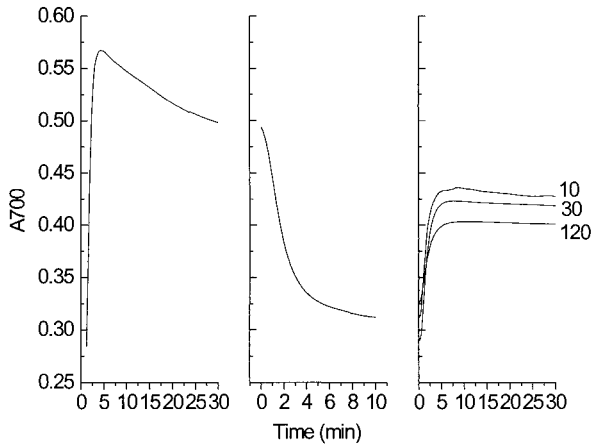

FIGURE 8 The aggregation, deaggregation, and reaggregation of 0.9 mM fluoromet Hb S in 0.75 M phosphate (pH 6.5), 0.44 M NaF, 0.14 M IHP. Raising the temperature of the sample holder from 10°C to 30°C induced aggregation and reaggregation, and deaggregation was induced by cooling from 30°C to 10°C. Sample turbidity was monitored at 700 nm.

To study the mechanism of FmetHb S polymerization we have monitored the effects of temperature, phosphate concentration, and Hb S concentration on the delay time. Based upon these data we conclude that many aspects of the polymerization of FmetHb S are analogous to aspects of the polymerization of deoxyHb S, and therefore, FmetHb S can be used to study the polymerization process. Furthermore, the stabilization of FmetHb S aggregates by IHP potentially provides a unique avenue for studying early events in the polymerization process and identifying factors that control the length of the delay time, a critical component in the pathology of sickle cell disease.

We thank Dr. Kenneth Bridges at Brigham and Women's Hospital for supplying SS blood samples. We gratefully acknowledge Jeff Gilarde for his assistance in preparing the grids and obtaining the electron micrographs of the FmetHb S fibers.

This work was supported by a grant-in-aid from the American Heart Association (GA 96015120).

REFERENCES

Adachi, K., and T. Asakura. 1982. Effect of liganded hemoglobin S and hemoglobin A on the aggregation of deoxy-hemoglobin S. *J. Biol. Chem.* 257:5738–5744.

Adachi, K., and T. Asakura. 1979. Nucleation-controlled aggregation of deoxyhemoglobin S: possible difference in the size of nuclei in different phosphate concentrations. *J. Biol. Chem.* 254:7765–7771.

Adachi, K., J. Kim, and N. Shibayama. 1991. Polymerization and solubility of Ni (II)-Fe(II) hybrid Hb S. *Biochim. Biophys. Acta.* 1079:268–272.

Antonini, E., and M. Brunori. 1971. Hemoglobin and Myoglobin and Their Reactions with Ligands. North Holland Publishing Company, London.

Behe, M. J., and S. W. Englander. 1978. Sickle hemoglobin gelation: reaction order and critical nucleus size. *Biophys. J.* 23:129–145.

Bookchin, R. M., and R. L. Nagel. 1971. Ligand-induced conformational dependence of hemoglobin in sickling interactions. *J. Mol. Biol.* 60: 263–270.

Briehl, R. W., E. S. Mann, and R. Josephs. 1990. Length distribution of hemoglobin S fibers. *J. Mol. Biol.* 211:693–698.

Coletta, M., P. Ascenzi, R. Santucci, A. Bertollini, and G. Amiconi. 1993. Interaction of inositol hexakisphosphate with liganded ferrous human hemoglobin. Direct evidence for two functionally operative binding sites. *Biochim. Biophys. Acta.* 1162:309–314.

Di Iorio, E. 1981. Preparation of ferrous and ferric hemoglobin. *Methods Enzymol.* 76:57–72.

Eaton, W. A., and J. Hofrichter. 1990. Sickle cell hemoglobin polymerization. *Adv. Protein Chem.* 40:63–279.

Fasanmade, A. A. 1996. Gelation kinetics of dilute hemoglobin form sickle cell anemia patients. *Blood.* 20:415–428.

Fermi, G., and M. F. Perutz. 1977. Structure of human fluoromethaemoglobin with inositol hexaphosphate. *J. Mol. Biol.* 114:421–431.

Ferrone, F. A., J. Hofrichter, and W. A. Eaton. 1985a. Kinetics of sickle hemoglobin polymerization. I. Studies using temperature-jump and laser photolysis techniques. *J. Mol. Biol.* 183:591–610.

Ferrone, F. A., J. Hofrichter, and W. A. Eaton. 1985b. Kinetics of sickle hemoglobin polymerization. II. A double nucleation mechanism. *J. Mol. Biol.* 183:611–631.

Harrington, D. J., K. Adachi, and J. William E. Royer. 1997. The high resolution crystal structure of deoxyhemoglobin S. *J. Mol. Biol.* 272: 398–407.

Hofrichter, J., P. D. Ross, and W. A. Eaton. 1974. Kinetics and mechanism of deoxyhemoglobin S gelation: a new approach to understanding sickle cell disease. *Proc. Natl. Acad. Sci. USA.* 71:4864–4868.

Hofrichter, J., P. D. Ross, and W. A. Eaton. 1976. Supersaturation in sickle cell hemoglobin solutions. *Proc. Natl. Acad. Sci. USA.* 73:3035–3039.

Huisman, T. H., and A. M. Dozy. 1965. Studies on the heterogeneity of hemoglobin. IX. The use of tris (hydroxymethyl) aminomethane-HCl buffers in the anion-exchange chromatography of hemoglobins. *J. Chromatogr.* 19:160–169.

Jayaraman, V., K. R. Rodgers, I. Mukerji, and T. G. Spiro. 1993. R and T states of fluoromethemoglobin probed by UV resonance Raman spectroscopy. *Biochemistry.* 32:4547–4551.

Juszczak, L. J., R. E. Hirsch, R. L. Nagel, and J. M. Friedman. 1998. Conformational differences in CO derivatives of HbA, HbC (Eβ6K) and HbS (Eβ6V) in the presence and absence of inositol hexaphosphate detected using ultraviolet resonance Raman spectroscopy. *J. Raman Spectrosc.* 29:963–968.

Mehanna, A. S., and D. J. Abraham. 1990. Comparison of crystal and solution hemoglobin binding of selected antigelling agents and allosteric modifiers. *Biochemistry.* 29:3944–3952.

Minton, A. P. 1983. The effect of volume occupancy upon the thermodynamic activity of proteins: some biochemical consequences. *Mol. Cell. Biochem.* 239:119–140.

Mozzarelli, A., J. Hofrichter, and W. A. Eaton. 1987. Delay time of hemoglobin S polymerization prevents most cells from sickling in vivo. *Science.* 237:500–506.

Padlan, E. A., and W. E. Love. 1985. Refined crystal structure of deoxyhemoglobin S. II. Molecular interactions in the crystal. *J. Biol. Chem.* 260:8280–8291.

Perutz, M. F., E. J. Heidner, J. E. Ladner, J. G. Beetlestone, C. Ho, and E. F. Slade. 1974. Influence of globin structure on the state of the heme. III. Changes in heme spectra accompanying allosteric transitions in methemoglobin and their implications for heme-heme interaction. *Biochemistry.* 13:2187–2200.

Riggs, A. 1981. Preparation of blood hemoglobins of vertebrates. *Methods Enzymol.* 76:5–29.

Ross, P. D., and A. P. Minton. 1977. Analysis of non-ideal behavior in concentrated hemoglobin solutions. *J. Mol. Biol.* 112:437–452.

Ross, P. D., and S. Subramanian. 1978. Ionic and non-ionic effects on the solubility of deoxyhemoglobin S. *In* Biochemical and Clinical Aspects of Hemoglobin Abnormalities. Academic Press, San Diego. 629–646.

Sokolov, L., and I. Mukerji. 1998. Conformational changes in FmetHbS probed with UV resonance Raman and fluorescence spectroscopic methods. *J. Phys. Chem. B.* 102:8314–8319.

Wellems, T. E., and R. Josephs. 1979. Crystallization of deoxyhemoglobin S by fiber alignment and fusion. *J. Mol. Biol.* 135:651–674.